

## **CHAPTER 4**

### **A NOVEL MAXIMUM POWER POINT TRACKING OF PV ARRAY USING SHORT CIRCUIT AND OPEN CIRCUIT VALUES FOR THREE-PHASE GRID CONNECTED INVERTER**

#### **4.1 INTRODUCTION**

Maximum Power Point Tracking (MPPT) is a mandatory segment in almost all PV systems. The commonly available MPPT techniques are implemented through DC-DC converters, which precede the grid side converter in the two stage converter interface. These MPPT algorithms normally return a duty ratio value to control the DC-DC converter for achieving Maximum power point (MPP). But when it comes to the control of inverters, these algorithms cannot be used directly unless they are modified suitably. This chapter proposes a novel MPPT technique which can be applied directly for voltage source inverters with a simple modification in the power circuit. Normally, in the grid connected converter control the power reference information for the inner current loop comes either from an MPPT algorithm or from a central control station as mentioned in chapter 3. This chapter proposes an MPPT technique which can directly give the power reference information for the inner current loops. The design, hardware implementation and testing of the proposed MPPT is presented in this chapter.

#### **4.2 NOVEL SHORT CIRCUIT CURRENT & OPEN CIRCUIT VOLTAGE MPPT**

The conventional MPPT methods proposed by Hohm & Ropp (2000), Esram et al. (2007), D'Souza et al. (2005) and Mastromauro Rosa et al. (2012)

like P&O, Incremental Conductance etc, are iterative numerical algorithms, demanding larger converging time before they reaches the maximum power point. The reason is that they have no initial knowledge of the maximum operating points at the start of iteration. The algorithm is initiated from some random low value of duty ratio for the dc-dc converter as revealed by Hohm & Ropp (2000) and Esham & Patrick (2007) and progresses through successive perturbations. Often in real time these algorithms fail to track the shift in operating points happening due to change in irradiance conditions or partial shading conditions as reported by Mastromauro Rosa et al. (2012). If the algorithm is made faster by increasing the perturbation intervals the optimum point is never reached. If the intervals are made smaller the algorithm has a sluggish response with oscillations around MPP. The proposed MPPT method tries to overcome these disadvantages by introducing a fast tracking algorithm without compromising on the accuracy of tracking.

The typical  $i-v$  characteristics of a solar module is given in Figure 4.1. The output current at the maximum power point is called the optimum current,  $I_{mpp}$  and when the output terminal is short circuited, the output current is called the short-circuit current,  $I_{sc}$ .

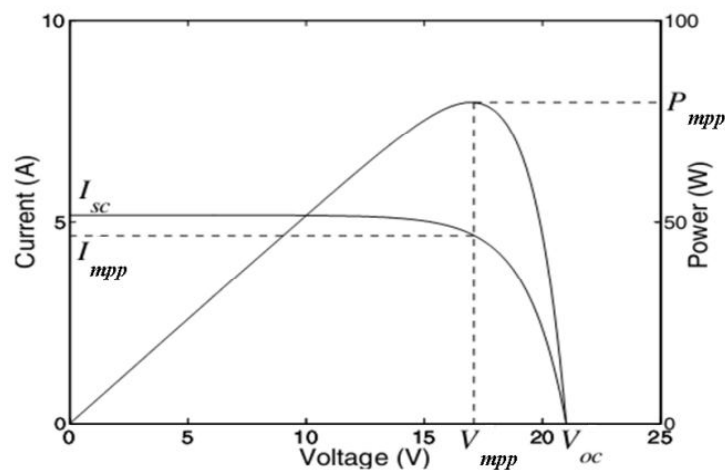


**Figure 4.1 Typical I-V Characteristics of a PV panel**

The relationship between  $I_{mpp}$  and  $I_{sc}$  is constant under any irradiance conditions for all PV panels. This unique feature of the PV panels is reported by Noguchi et al.(1998), (2000), (2003), Lee et al. (2003), Kobayashi et al. (2004) and Scarpa et al. (2009). It can be verified theoretically by observing the values of  $I_{sc}$  and  $I_{mpp}$  values from the datasheets of the solar PV modules listed in the reference for UniSolar PVL-68 and Mitsubishi PV-MLT 260HC.

An attempt is made to find the relationship between  $I_{mpp}$  and  $I_{sc}$  experimentally, by conducting load test and short circuit tests of some of the available PV panels by maintaining the insolation conditions the same. The results show that the ratio between these two currents will remain a constant ( $k_i$ ) for a given panel of any make, model and rating under all irradiance and temperature conditions. Experiments were conducted on two different PV panels Unisolar PVL68 and Mitsubishi PV-MLT 260HC. The results of these tests under various irradiance conditions are consolidated in Table 4.1a & 4.1b. The same relationship is verified by various authors in the literatures as well.

$$I_{mpp} = k_i I_{sc} \quad @ \text{ any } G \quad (4.1)$$

Where  $k_i$  is the proportionality constant for short circuit current, and  $G$  is the irradiance. The experimental results are plotted and shown in Figure 4.2, which shows that the graph between  $I_{sc}$  Vs  $I_{mpp}$  is straight lines for commercial PV panels. This means that  $k_i$  is a constant. Therefore from equation (4.1) the MPP current can be estimated at any instant of our interest by knowing the short circuit current and the constant  $k_i$ .

Similarly referring to Figure 4.1 the output voltage of the PV panel when it delivers maximum power is called the optimum voltage  $V_{mpp}$  and

when the output terminals are open circuited, the output voltage is called open circuit voltage  $V_{oc}$ .

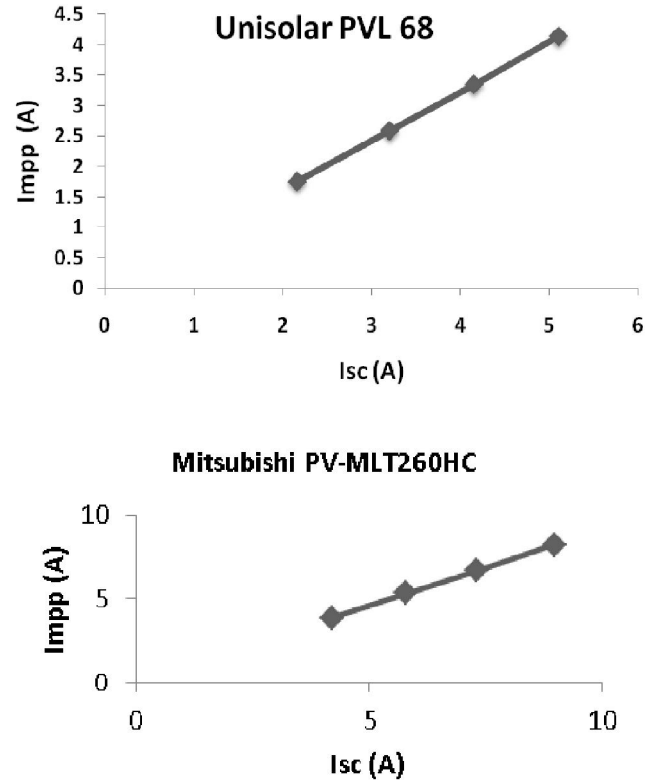


**Figure 4.2** Experimental results of  $I_{SC}$  Vs  $I_{mpp}$

Studies and experiments were carried out to assess whether a similar relationship like the currents does exist between the open circuit voltage,  $V_{oc}$  and voltage at maximum power point  $V_{mpp}$ . i.e. the ratio between  $V_{oc}$  and  $V_{mpp}$  will it remain constant for a given PV panel under all irradiance conditions. If such a relationship exists then estimation of the Maximum power value will be very simple and which can act as a reference for the power converter's controller which may ensures that the entire available power is transferred in to the grid.

The expected relationship between the voltages of a PV array is presented as,

$$V_{mpp} = k_v V_{oc} \quad @ \text{ all } G \quad (4.2)$$

Where  $k_v$  is the proportionality constant for open circuit voltage, and  $G$  is the irradiance.

**Table 4. 1.a Experimental estimation of  $k_i$  and  $k_v$  values for Unisolar PVL 68**

<b>Irradiance (W/m<sup>2</sup>)</b>	<b>V<sub>oc</sub> (V)</b>	<b>I<sub>sc</sub> (A)</b>	<b>I<sub>mpp</sub> (A)</b>	<b>V<sub>mpp</sub> (V)</b>	<b>k<sub>i</sub></b>	<b>k<sub>v</sub></b>
1000	23.1	5.1	4.13	16.5	0.809	0.714
800	22.8	4.15	3.34	16.3	0.805	0.714
600	22.6	3.2	2.58	16.16	0.806	0.715
400	22.5	2.1	1.75	16.1	0.809	0.715

The same experiments as conducted for obtaining the current relationship is executed along with the open circuit voltage measurements under various illumination conditions. The results were consolidated in Table 4.1.a and 4.1.b. From Table 4.1 it can be found that there exists a linear relationship between  $V_{oc}$  and  $V_{mpp}$ . The experimental results are plotted and shown in Figure 4.3, which shows that the graphs between  $V_{OC}$  Vs  $V_{mpp}$  are also straight lines for typical panels. To conclude, the values of  $k_i$  and  $k_v$  are constant over the entire range of practical irradiance.

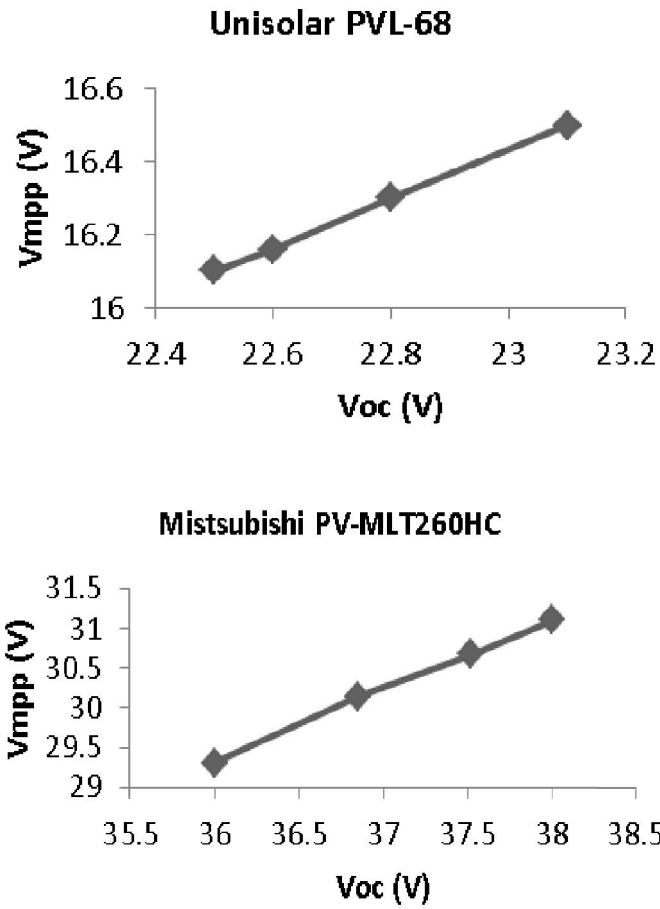


Figure 4.3 Experimental results of  $V_{OC}$  Vs  $V_{mpp}$

Table 4.1.b Experimental estimation of  $k_i$  and  $k_v$  values for Mitsubishi PV-MLT260HC

Irradiance ( $W/m^2$ )	$V_{oc}$ (V)	$I_{sc}$ (A)	$V_{mpp}$ (V)	$I_{mpp}$ (A)	$k_i$	$k_v$
1000	38	8.98	31.1	8.25	0.919	0.82
800	37.52	7.3	30.67	6.71	0.920	0.817
600	36.85	5.8	30.14	5.34	0.921	0.818
400	36	4.2	29.30	3.86	0.921	0.814

To validate the generality of these relationships under partial shading conditions, experiments were conducted creating intentional partial shadings and the results are presented for one worst partial shading condition in Table 4.2. A small reduction in the  $k_v$  and  $k_i$  values were observed, but the error in the power value varied between 5% to 20% for a light partial shading to a worst partial shading. It is also observed that the common partial shadings like cloud passing lasts only for a few seconds and the power variations are less than 10 %.

**Table 4.2 Experimental estimation of  $k_i$  and  $k_v$  values for UnisolarPVL 68 under partial shading**

<b>Irradiance (W/m<sup>2</sup>)</b>	<b>V<sub>oc</sub> (V)</b>	<b>I<sub>sc</sub> (A)</b>	<b>I<sub>mpp</sub> (A)</b>	<b>V<sub>mpp</sub> (V)</b>	<b>k<sub>i</sub></b>	<b>k<sub>v</sub></b>
1000	21.1	3.8	2.96	15.0	0.780	0.711
800	20.8	3.21	2.53	14.79	0.787	0.711
600	20.1	2.97	2.33	14.23	0.784	0.708
400	19.5	1.98	1.54	13.79	0.778	0.707
200	19.2	1.01	0.78	13.54	0.771	0.705

Thus in a PV panel, if the  $I_{sc}$  and  $V_{oc}$  values are measured online during the operation at periodic intervals and values of  $k_i$  and  $k_v$  of the panel are known, the maximum power points of the panel can be obtained with a reasonable accuracy as,

$$\begin{aligned}
 P_{mpp} &= V_{mpp} I_{mpp} \\
 P_{mpp} &= k_i k_v V_{oc} I_{sc}
 \end{aligned}
 \tag{4.3}$$

The estimated  $P_{mpp}$  will serve as the power reference for the inverter controller. The proposed algorithm calculates the power from the periodically sensed values of OC voltage and SC current. The  $V_{OC}$  and  $I_{SC}$  values are to be sensed at a rate much higher than the rate at which the changes happen in the ambient conditions. This results in a better maximum power point tracking accuracy and efficiency. The algorithm is inherently immune to shifts in operating points due to partial shading as well as irradiance changes because the power output of solar PV cell is directly proportional to the current which in turn is proportional to the irradiance on the panel. The speed of this algorithm depends on the response of the PV panel and the response of the current and voltage transducers that periodically sense  $V_{oc}$  and  $I_{sc}$ . Thus the proposed MPPT technique is best suitable for fast changing environmental conditions as it can track and account the power variations due to irradiance changes including the partial shading conditions.

### 4.3 SYSTEM DESCRIPTION

The power circuit consists of a three phase voltage source inverter (VSI), the output filter and the controlled turn on and off switches for obtaining the OC and SC conditions online of the PV panel as shown in Figure 4.4. Switch S1 is the series switch which open circuits the panel from feeding the inverter, and switch S2 the shunt switch which short circuits the panel provided when S1 is open. Under normal operating conditions, S1 will remain ON and S2 is OFF. Whenever the power reference is to be updated by sensing of the panel quantities then, the hierarchy in which the switches are operated is as follows: first S1 is made OFF from its normally closed condition, and then S2 is made ON from its normally open condition. Conversely, while restoring back to the normal operating condition, first S2 is turned OFF, then S1 is made ON. A current transducer and a voltage transducer are connected as shown in Figure 4.4 to sense the current and

voltage of the panel. The design details of the current and voltage sensing circuits are appended in Appendix 3.

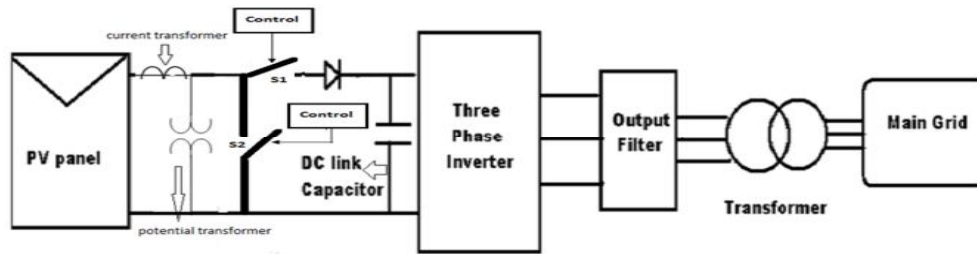


**Figure 4.4 The power circuit of the proposed MPPT system**

Periodically when, S1 is opened for a short duration, the PV array is open circuited and the voltage is sensed and is received by the micro-controller, wherein the control is implemented. During S1's off period, when S2 is made on, it will result in a short circuit across the output of the PV panel for a small period, and the sensed short circuit current is received by the micro-controller.

The PV panel is a 68Wp flexible multi-junction Unisolar PVL-68 whose datasheet is listed in the reference list, with eight of them connected in series for a power rating of 500W. Both S1 and S2 are power MOSFETs rated to withstand the open circuit voltage of the panel and to carry the short circuit current of the panel continuously. A fast recovery diode is connected in series with S1 to prevent the capacitor from discharging through the body diode of S1 during short circuiting period. A dc link capacitor is selected and used at the input of the inverter to maintain the input voltage constant even when the panel is disconnected from the inverter for MPPT. An output filter after the inverter is used to remove the switching frequency components of the inverter output to result in a sinusoidal output voltage and current. A three phase transformer is used at the output of the inverter to step up the output voltage to the standard grid value before feeding it to the grid.

### 4.3.1 Design of dc Link Capacitor

The DC link capacitor is connected at the input of the three phase inverter to maintain the dc voltage constant. The dc link voltage at the output of the panel can have a maximum value of 152V at a power rating 500W. Hence the voltage rating can be anything greater than 152 V say 200 V. The capacitance value should be designed from the total time for which the panel is disconnected from the inverter during which it has to support the energy requirements of the inverter. However, the disconnection duration is influenced by the time constant of the panel i.e the time taken by the PV panel to rise to its short circuit current value, and to open circuit voltage from its normal working condition.

The implementation of the control scheme in real time requires, testing of the available UNISOLAR PVL68 to find out its time constant upon a short circuit and open circuit. An experiment is conducted with a simple test circuit shown in Figure 4.5 (a) to test the panel. The test was conducted under different light conditions and the observed results showed that the time taken by the PV panel to rise to the short circuit current varied from 100 $\mu$ s to 320 $\mu$ s. The waveform in Figure 4.5 (b) shows the transition of PV panel's current from open circuit to short circuit condition under very low, light condition around 220 W/m<sup>2</sup>. This is the highest recorded time for the transition by the panel.

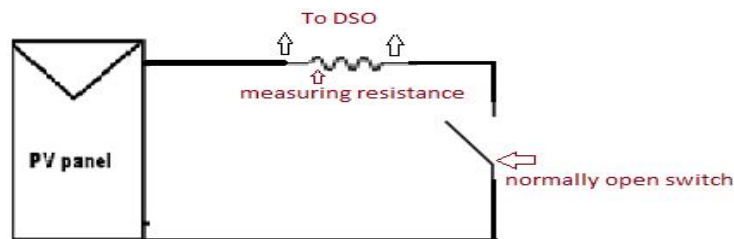


**Figure 4.5 (a) Test circuit to measure PV panel time constant**



**Figure 4.5 (b) Transition of PV panel current from OC to SC**

Similarly around 70  $\mu\text{s}$  to 110  $\mu\text{s}$  is found required for the panel to reach the open circuit voltage from the normal working voltage. So the series switch must be turned off at least for a duration of 430  $\mu\text{s}$  to complete the sensing process.

For calculation of the capacitor value the duration of the series switch to remain open is taken as 1ms which is far greater than the minimum time required. During this period the drop in voltage is to be limited to 5% of the initial value as,

$$\left[ \left( \frac{1}{2} C V_1^2 \right) - \left( \frac{1}{2} C V_2^2 \right) \right] = P T_{on} \quad (4.4)$$

Where  $V_1=155\text{V}$ ,  $V_2=147\text{V}$ ,  $P=500\text{W}$  and Series switch open time  $T_{on}=1\text{ms}$ . From equation (4.4) the value of capacitance was found out to be,  $C = 413\mu\text{F}$ . A capacitor rated at 200V, 500 $\mu\text{F}$  is used as a dc link capacitor in the prototype.

### 4.3.2 Output filter design

The output LC filter is designed with the assumption that the reactive power absorbed by the capacitor is 5% of the rated power for a switching frequency of 1 kHz. Though the current regulated PWM has a variable switching frequency, 1 kHz is the lowest observed frequency found from simulation studies. The value of capacitor and inductor was determined to be 2.4 $\mu$ H and 11mH respectively.

### 4.3.3 Fast recovery diode selection

A fast recovery diode is used in series with the switch S1 in the power circuit before the dc link capacitor. This diode is connected to ensure that the dc link capacitor does not discharge through the body diode of the series switch S1 during short circuit. This may result in an erroneous value of  $P_{mpp}$  by the algorithm. Also, the reverse recovery current of the diode during off state should be very low so that the accuracy of the sensed  $I_{sc}$  would be high. Considering all these details a MOSFET switch is used as a diode by short circuiting its gate and source terminals.

### 4.3.4 Specifications of the three phase inverter

An intelligent power module of two back to back three phase bridge inverter stack manufactured by SEMIKRON is used for the implementation of the power circuit. It has an inbuilt driver and isolation circuits. The supply specifications are:

Maximum input AC voltage up to 415 Volts 3-phase

Maximum switching frequency up to 20 kHz PWM

A 15 V DC to be applied for the internal driver circuits and an amplification circuit to amplify the output pulses of microcontroller are also necessary as an auxiliary circuit.

### 4.3.5 Microcontroller Specifications

The dsPIC30F3011 microcontroller from Microchip is used for implementing the current controller as well as the short and open circuit switch timing control. The major features of the microcontroller are 16 bit modified Harvard architecture, built in DSP engine, 24kB on-chip flash program space, 1kB on-chip RAM, 1kB data EEPROM, up to 30 MIPS operation, integrated peripherals like ADC, MCPWM, and Input Capture etc. The dsPIC30F3011 controller board is designed with 20 MHz crystal oscillator. The timer module, ADC module and PWM module of the dsPIC30F4011 are utilized to implement the proposed algorithm. The synchronised switching pulses are obtained by using the interrupt modules in dsPIC processor. The PWM module of the dsPIC generates the switching pulses to the inverter, by comparing the captured actual current and the calculated reference current.

## 4.4 CONTROL STRATEGY FOR INVERTER IN THE PROPOSED MPPT SCHEME

The inverter of the proposed system is controlled using hysteresis current controller. The block diagram of the inverter control is presented in Figure 4.6 and it is a combination of sinusoidal hysteresis current controller and the proposed MPPT using information from the panel side ( $V_{oc}$ ,  $I_{sc}$ ,  $k_i$  and  $k_v$ ) as well as the information from the grid side (grid voltage magnitude and phase) to ensure power transfer from the PV panel to the grid with a single power converter at unity power factor. The first stage involves the calculation of the maximum power  $P_{mpp}$  available from the panel at any instant using the MPPT. Assuming ideal conditions for the power converter the power equation of the system is written as,

Power at dc side = Power at ac side

$$P_{mpp} = V_{mpp} I_{mpp} = \sqrt{3} v_{LL} i_{LL} \cos \varphi$$

$$P_{mpp} = k_i k_v V_{oc} I_{sc}$$
(4.5)

Where  $v_{LL}$  is the Line to line voltage of the grid and  $i_{LL}$  is the rms current to be delivered for transferring the available power  $P_{mpp}$ . If the magnitude of the grid voltage  $v_{LL}$  is sensed from the point of common coupling between the inverter output and the grid, then the equivalent peak ac current that should flow at the inverter output to deliver the power available from the panel  $I_m$  can be calculated as,

$$I_m = \frac{P_{mpp}}{v_{LL}} \left( \frac{\sqrt{2}}{\sqrt{3}} \right)$$
(4.6)

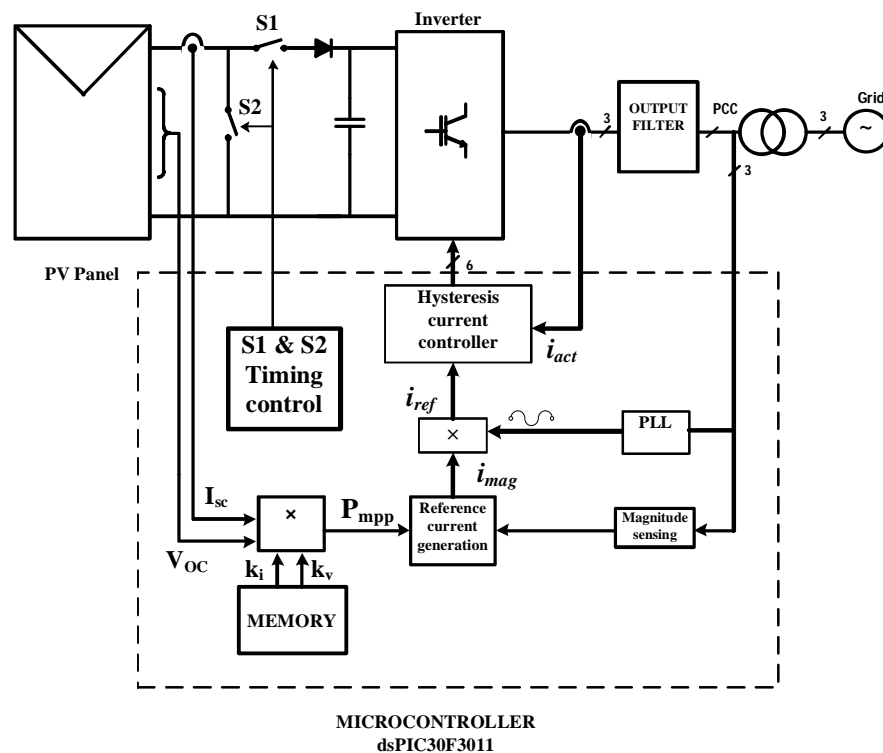


**Figure 4.6 MPPT control of Inverter through current control**

A unit magnitude sine wave which is in-phase with the grid voltage is generated using a Phased Locked Loop (PLL) as explained in chapter 3 and the reference current  $I_{ref}$  for the hysteresis current controller is obtained by multiplying the magnitude from equation (4.6) with the unit sine wave. This will ensure that the current is delivered at unity power factor at PCC. These reference current waveforms are then compared with actual line currents by the sinusoidal hysteresis current controller and subsequently the gate pulses are generated. In a sinusoidal band controller, the hysteresis band varies sinusoidally over the fundamental period, as shown in Figure 4.7 while the control band varies as

$$i_{ref} = I_m \sin \omega t \quad (4.7)$$

$$i_{up} = (i_{ref} + H) \sin \omega t \quad (4.8)$$

$$i_{low} = (i_{ref} - H) \sin \omega t \quad (4.9)$$

Where H is the hysteresis band taken as 5% of  $i_{ref(rms)}$  for this research work. The typical inverter output voltage corresponding to the current control is shown in Figure 4.8.

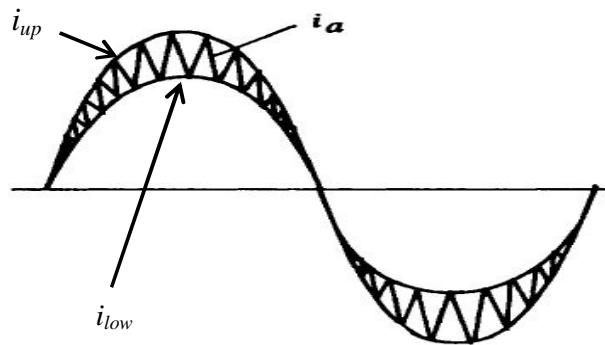


**Figure 4.7 Sinusoidal band hysteresis current controller output**

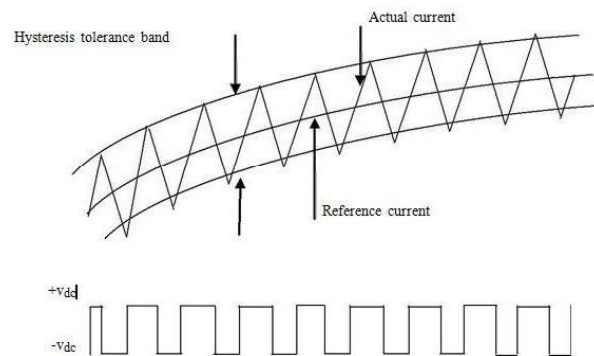


**Figure 4.8 Hysteresis current controlled inverter output voltage**

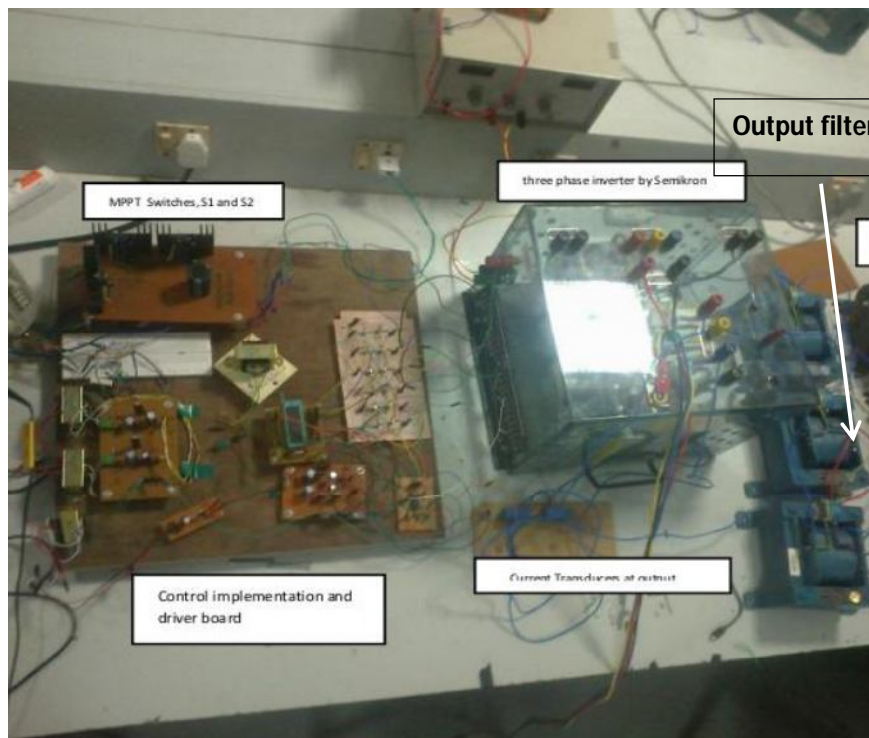
Current controllers are preferred over voltage based controllers because they have faster response, provide inherent over current protection to power circuit switches and improves the fault tolerance of the system as conferred by Ned Mohan et al. (2007) and Bose (1990). The advantage of this control scheme is that it implements MPPT in single stage power interface while maintaining all features of a current based control strategy.

The timing control of the series and shunt switches and the current reference generation with gating signals generation follow a master slave sequence where the outer master loop produces switching pulses for S1 and S2 once in every three seconds. The rate of obtaining the  $V_{oc}$  and  $I_{sc}$  is decided to be 3s considering the fact that the changes in the ambient conditions like change in light due to cloud passing, temperature changes etc., typically take several seconds. The switching is done such that the shunt switch S2 is switched on for a period of  $350\mu s$  after opening the series switch S1. S1 is kept open for  $600\mu s$  slightly higher than the time delays for the PV measurements to account for the sensor delays. Within  $600\mu s$  both the open circuit voltage and the short circuit current are sensed. Hence once in every 3s a new MPP power rather a power reference is calculated and the panel's operating point is updated. For all practical implementations this period can

be further increased up to 10s depending on the site conditions without any loss in speed or accuracy of the algorithm.

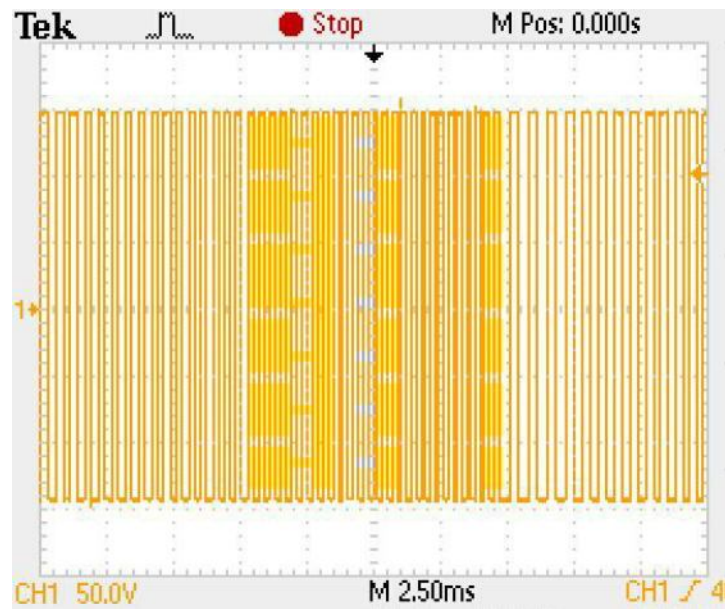
#### 4.5 EXPERIMENTAL RESULTS & PERFORMANCE OF THE PROPOSED MPPT

The experimental setup of the entire system excluding the PV panels is shown in Figure 4.9. The experiment is conducted with the proposed algorithm on different days with different irradiance as a field trial.

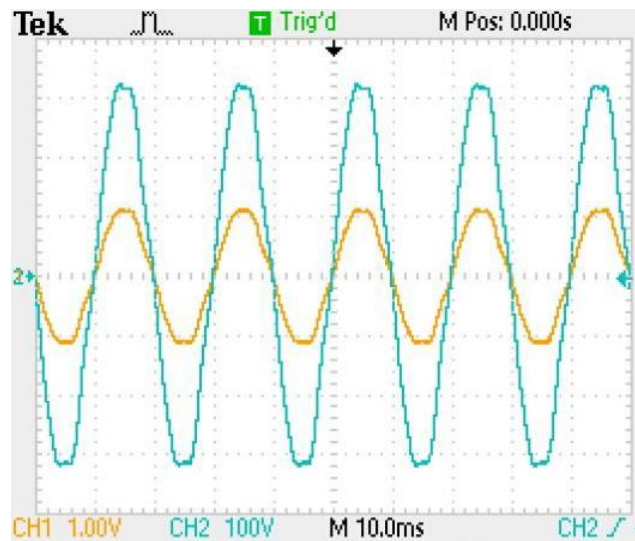


**Figure 4.9** The experimental setup of the proposed MPPT

Figure 4.10 shows the inverter output voltage. Figure 4.11 shows the voltage and current at the point of common coupling while the irradiance is recorded in the meter as  $1100 \text{ W/m}^2$ . It is found that the current delivered by the inverter is 1 A peak. Also it can be noted that the current delivered is in phase with the voltage.



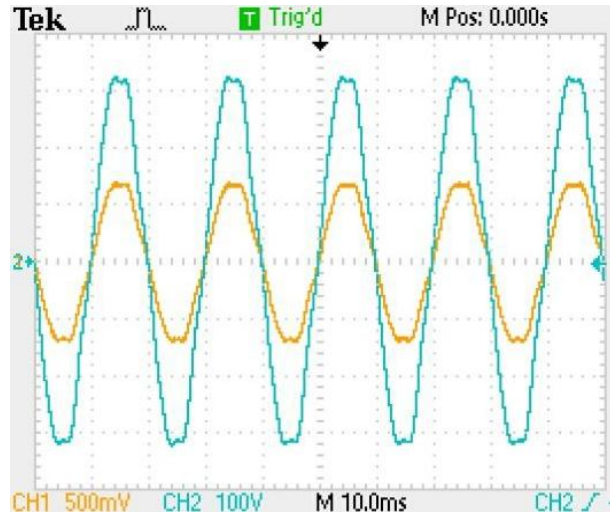
**Figure 4.10 Inverter output voltage**



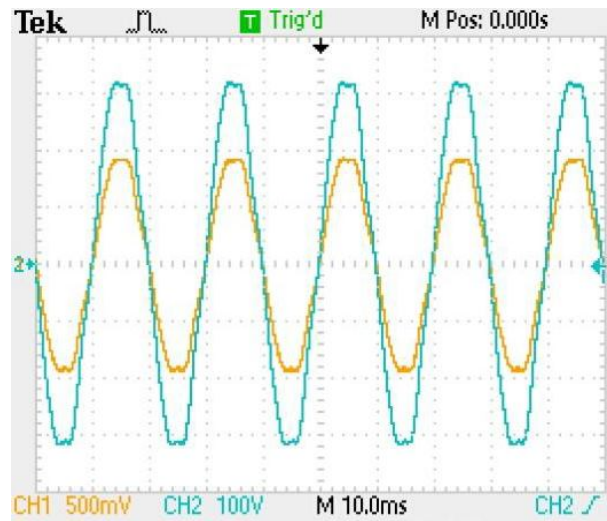
**Figure 4.11 Voltage and current at PCC for 1100 W/m<sup>2</sup>**

Figure 4.12 shows the voltages and current delivered by the inverter for a recorded irradiance of 639 W/m<sup>2</sup>. Here also the current is delivered at UPF with amplitude of 0.68A. The same is repeated with another irradiance of 873 W/m<sup>2</sup>

wherein the current amplitude is found to be 0.95A as shown in Figure 4.13. In all the cases the current THD is found to be within 5%.



**Figure 4.12 Voltage & current at PCC for 639 W/m<sup>2</sup>**



**Figure 4.13 Voltage & current at PCC for 873 W/m<sup>2</sup>**

To verify whether the proposed algorithm takes care of the partial shading conditions, intentional partial shading is created when the recorded

irradiance is  $950 \text{ W/m}^2$ . Under this condition, load test is conducted on the PV array resulted a  $P_{\text{mpp}}$  of 274 W. With the same condition the current delivered by the inverter is observed and presented in Figure 4.14. It is found that the amplitude of the current delivered is 0.53 A, corresponds to a power of 269 W. This complies with the available  $P_{\text{mpp}}$  of 274 W considering the non-linearity of the constants under partial shading. This can be justified as 2% reduction in power because of the deviation in the OC & SC constants due to partial shading.

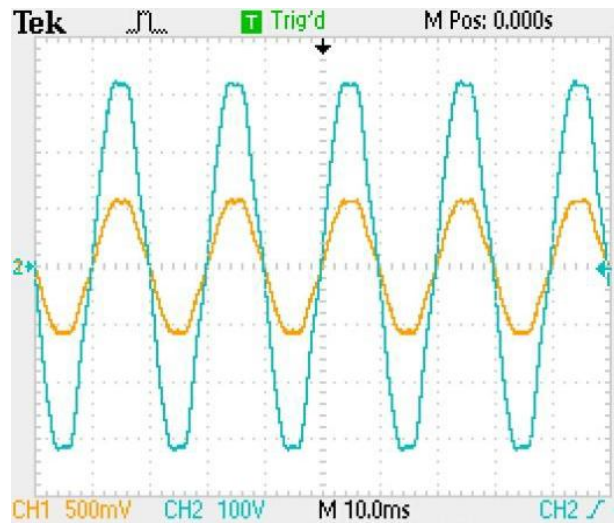


**Figure 4.14 Voltage and current at PCC under partial shading condition.**

#### 4.6 CONCLUSION

This chapter presented the design, development and hardware implementation of a single stage power electronic interface for transfer of power from photovoltaic (PV) panel to the grid using a current controlled voltage source inverter with a novel non-iterative maximum power point tracking (MPPT) method. The power at maximum power point is obtained by sensing the  $V_{\text{OC}}$  and  $I_{\text{SC}}$  online from the panel during operation. A sinusoidal

band hysteresis current controller receiving the current reference calculated from the  $P_{mpp}$  and is used for switching the inverter. The results from the experimental setup under different irradiance conditions are presented and verified for partial shading condition also. The verification of the power values found by the proposed MPPT algorithm by conducting conventional load tests and compliance is confirmed. The convergence speed of this algorithm is superior as it is a non-iterative method of MPPT and the oscillations around the optimum operating point are not felt. A small deviation in the OC and SC constant values under partial shading conditions can be tackled by incorporating a hill climbing iteration of the reference current from the calculated value as a future progression for the algorithm. The convergence speed will not be affected as there is an initial knowledge of the maximum operating point at the start of iteration with this MPPT unlike other MPPTs that start from a random operating point. This algorithm can be implemented with the SRF current controller of chapter 3 to provide active power reference for the inner current loop.